EDITORIAL BOARD

ADVISORY BOARD

EDITORIAL

Introduction of Optics in Physical Sciences for better system response.

SOURANGSHU MUKHOPADHYAY

From the early days of civilization conscious people have given their effort more and more for introducing optics in physical explanations, behaviours, analyses and studies, because of the tremendous advantages hidden in optical signal over all the other signals. These advantages are being now exploited (and explained) in parallel processing, parallel computation, high power generation, intelligent functioning of systems, production systems, robotics, information and communication technologies, and many other scientific fields. Superfast operational speed in those areas can be achieved very successfully by proper introduction of optics. Performances in point of view of the removal of all sorts of complexities, and all, other responses from an all-optical/opto-mechanical/opto-electronic system can not be compared at-al with the conventional counter-parts of these operational systems. The interactions between man, machine and optics are being strengthened and signified more and more to get the best responses of the systems for best functioning. Future world will use 'optics' in each of its step to deal physical systems for greater horizon.

— o —

Opto-Electronic Conductance in ZnTe Film

S. Bandyopadhyay & S.K. Ghorai

Department of Physics and Techno-Physics
Vidyasagar University,
Midnapore, West Bengal 721 102. India

INTRODUCTION:

'Slow relaxation' is one of the most interesting photoelectronic effects in Semiconductors, which is manifested by anomalously long relaxation time of photo-response at the beginning or end of illumination. Residual Conductivity is the special case of slow relaxation, which is manifested by the retention of relatively high conductivity for a long time after the cessation of photoative illumination. The self evident nature of the potential practical applications like optoelectronic memory elements, vidicons etc., and the physical nature of the phenomena involved, are the main factors that have drawn our keen interest in slow relaxation and residual conductivity in some semiconductor thinfilms like ZnTe film with and without doping. In this note some relevant parameters for three different thickness of the film and the variation of conductance with temperature are presented.

Film Preparation and Conduction measurements :

Films of ZnTe of different thickness are deposited on glass substrates as usual, in a vacuum of the order of 10^{-4} pa at room temperature (298 K). For doping, the films of nearly 600 nm thickness are deposited at a substrate temperature of 573 K.A fixed amount of dopant like $PbC1_2$ (6% W/W), BaF_2 (7% W/W) and In (6% W/W) are deposited on the surface of ZnTe films, and then the films are annealed as necessary in proper way. For all the sets the deposition rate is maintained at ~120 nm/ minute. The thicknecesses of the film are measured with a surfometer as well as by interferometry. The photoconductance measurements at different temperatures are usually done using a cryostatic arrangement. The conductivity measurement of ZnTe films in dark and under illumination are carried out within the range of 140 K - 373 K temperature. A tungsten halogan lamp (600 W-230 V) fed by a constant voltage supply is used as the source of white light. The spectral response of photoconductivity is measured with the help od an Oriel monochromator (Model No. 77250). Relaxation of conductivity after the cessation of photoexcitation is recorded by an omniscribe strip chart recorder (Model No. 5000). For all the conductivity and decay measurements graphite paint (aqua-dag) is used for the ohmic contacts.

Computation of different parameters :

After measuring the temperature variation of dark and photo-conductance for doped ZnTe films of different thicknesses we can determine the values of ϕ_r, $\phi_d+(E_F-E_V)$ and $\phi_d - (\phi_{ro}+E_F - E_V)$ from the slopes of corresponding graph plots. Here ϕ_r is the recombination barrier height and ϕ_{ro} is the barrier height in dark. ϕ_d is termed as the barrier height. E_F and E_V are respectively the Fermi level and top of the valence band.

The following is the tabulation of different electrical parameters of undoped ZnTe films of different thickness deposited at room temperature (298 K).

Sample	Thickness t (nm)	$\phi_d+(E_F-E_V)$ (eV)	$\phi_d-(\phi_{ro}+E_F-E_V)$ (eV)	$\phi_{ro}+(E_F-E_V)$ (eV)	ϕ_d (eV)	E_F-E_V (eV)	ϕ_{ro} (eV)
Undoped ZnTe film	420	0.51	0.32	0.13	0.45	0.06	0.07
(T_S=298K)	630	0.80	0.45	0.30	0.75	0.05	0.25
	870	0.95	0.50	0.40	0.90	0.05	0.35

Conclusion :

From the experiment it is emphasized that mode of decay under weak and moderate illumination intensities are different, and the decay process is very sensitive to the temperature. Experimental results show that the recombination barrier is different from the grain-boundary drift barrier, the height of which is assumed not to be modulated under illumination.

Acknowledgement :

The authors thank to Prof. A. K. Chaudhuri, I. I. T., Kharagpur for his kind co-operation.

References :

1. **G. M. K. Thutupalli,** *et al, J. Phys. D : Appl, Physics.* 9, **1639,** 1976.
2. **T. L. Chu,** *et al, J. Appl. Phys.* 59, **1259,** 1986.
3. **A. Mandal,** *et al, Appl. Phys.* A. 43, **81,** 1987.
4. **U. Pal,** *et al, Phys. Stat. Sol. 111,* **532,** 1989.
5. **A. K. Chaudhuri, S. K. Ghorai,** *Solar Cell,* Modern Book Agency, 1992.
6. **U. Pal, D. Samanta, S. Ghorai,** *J. Phys. D. Appl. Phys.* 25 **1488,** 1992.
7. **U. Pal, D. Samanta, S. Ghorai,** *J. Appl. Phys.* 74, **10,** 1993.

Fig. 1 shows the variation of $\phi_d-(\phi_{ro}+E_F-E_V)$ with thickness (t) for undoped ZnTe film deposited at T_S=298K (room temperature). Fig. 2 shows the temperature variation of dark and photoconductance of a BaF_2 doped (7% W/W) ZnTe film (660 nm) deposited at 573 K.

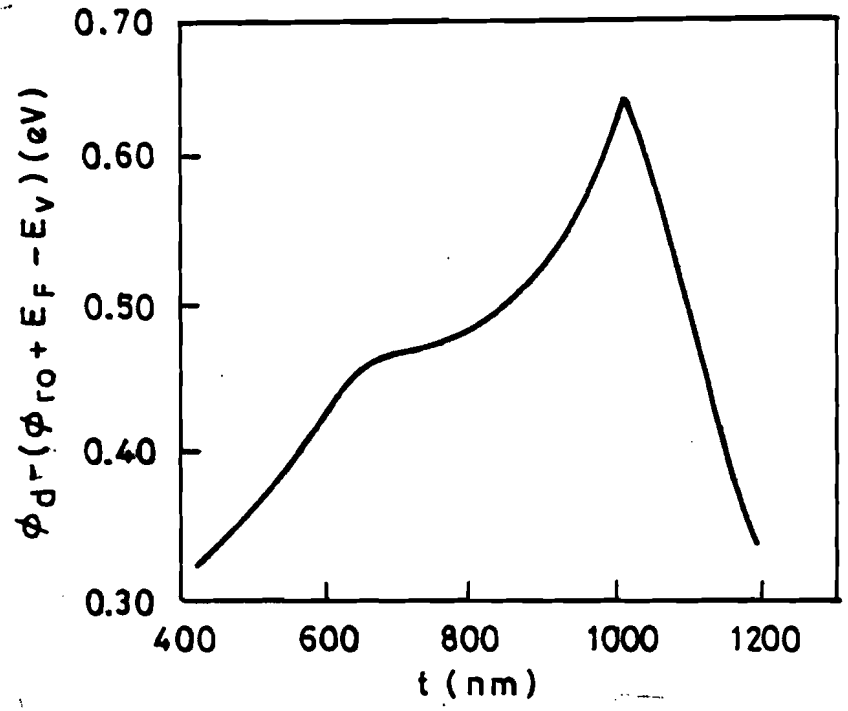
0.70
0.60
0.50
0.40
0.30
$\phi_{dr}(\phi_{ro}+E_F-E_v)$ (eV)
400
600
800
1000
1200
t (nm)

Fig. 1

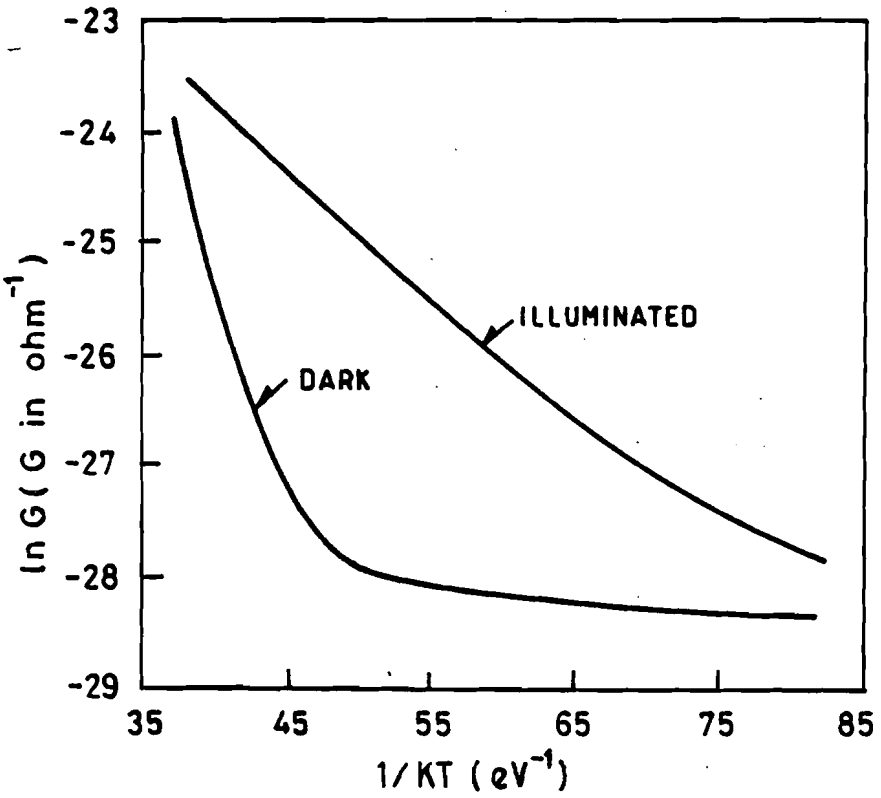
-23
-24
-25
-26
-27
-28
-29
ln G(G in ohm^{-1})
ILLUMINATED
DARK
35
45
55
65
75
85
1/KT (eV^{-1})

Fig. 2

A New Method of Solving Werners's Fuzzy LPP

T. Hossain
Sabang College, Vidyasagar University

T.K. Pal
Deptt. of Applied Mathematics, Vidyasagar University

Abstract : An alternative method of solving the fuzzy linear programming problem of Werners is presented here with the help of introducing effective constraints. Each fuzzy constraint is replaced by a crisp effective constraint formed by combining the constraint and its tolerance limits with the objective function and thereby reducing the number of crisp constraints in the equivalent nonfuzzy LPP.

1. INTRODUCTION :

Werners [2,3] considered LPP whose constraints are fuzzy with given tolerance limits. According to him the fuzzy behaviour of the constraints also makes objective function fuzzy. Werners considered the two optimum values of the crisp objective function corresponding to the two feasible regions obtained by taking lower and upper tolerance limits of the constraints to form the membership function of the fuzzy set for this fuzzy objective function. Max-min operator of Bellman and Zadeh [1] are then used to the membership functions of both fuzzy constraints sets and fuzzy objective function set to find the decision of the fuzzy problem. In this paper a new method of solving the same fuzzy LPP is developed with the use of effective constraints. Corresponding to each fuzzy constraint an effective constraint is formed with the help of the constraint itself, its tolerance limits and the objective function. An equivalent crisp LPP is thus formed giving the same solution as given by Werners's method. As the number of constraints and variables in the equivalent crisp LPP of this method is less than those in the Werners's method the optimal solution is obtained in less number of steps of simplex method and thus reducing considerable computational time. For illustration of this method two examples are considerd.

2. DEFINITIONS AND RESULTS OF WERNERS :

The classical crisp LPP is

Maximize $z = cx$

subject to $A x \leq b$ and $x \geq o$ (2.1)

where c and x are n-vectors, b is an m-vector (unrestricted is sign) and A is an m x n matrix.

Werners[3] considered the following LPP with fuzzy constraints.

Maximise $z = cx$

subject to $Ax \lesssim b$ and $x \geq o$ (2.2)

where "fuzzy less than or eual to" "$\lesssim$" denote the fuzzified version of "$\leq$" having linguistic interpretation as essentially smaller than or equal i.e. $(Ax)_i$ is about b_i or less for each i.

The fuzziness of the ith (i=1,2,.....,m) constraint over the tolerance range $[b_i, b_i + p_i]$ is characterised by the linear membership function $\mu_i(x)$ as

$$\mu_i(x) = \begin{cases} 1 & \text{if } (Ax)_i < b_i \\ [p_i + b_i - (Ax)_i]/p_i & \text{if } b_i \leq (Ax)_i \leq b_i + p_i \\ 0 & \text{if } (Ax)_i > b_i + p_i . \end{cases}$$

According to Werners because of the fuzzy behaviour of the constraints the objective function should also become fuzzy. To get the membership function for this fuzzy objective Werners first defind m and m+m' as follows

$m = \max cx$

subject to $(Ax)_i \leq b_i$ i =1,2,.....,m

and $x \geq o$

and

$m + m' = \max cx$

subject to $(Ax)_i \leq b_i + p_i$, i =1,2,.....,m

and $x \geq o$.

Using m and m' the membership function of the fuzzy objective function is defind as

$$\mu_0(x) = \begin{cases} 1 & \text{if } cx > m + m' \\ (cx - m)/m' & \text{if } m \leq cx \leq m+m' \\ 0 & \text{if } cx < m. \end{cases}$$

The optimum solution of this fuzzy LPP is obtained by using Bellman-Zadeh's max-min operator as follows

$\max \alpha(x)$ where $\alpha(x) = \min \{\mu_0(x), \mu_1(x), \mu_2(x), \ldots\ldots\ldots\ldots, \mu_m(x)\}$

$x \geq o$.

The crisp formulation of this problem is

Maximize α

subject to $\mu_i(x) \geq \alpha$, i = 0,1,2,.....,m

$0 \leq \alpha \leq 1$

and $x \geq o$.

i.e. Maximize α

subject to $cx - m' \alpha \geq m$

$(Ax)_i + p_i \alpha \leq b_i + p_i$, i = 1,2,3....., m (2.3)

$0 \leq \alpha \leq 1$ and $x \geq o$.

3. Development of the proposed method.

3.1 Construction of effective constraints.

Let m and m+m' be the maximum values of the objective function respectively for $Ax \leq b$, $x \geq o$ and $Ax \leq b + p$, $x \geq o$.

The maximum profit hyperplanes of these two LPP are then $cx = m$ and $cx = m + m'$ and the corresponding hyperplanes arising from the ith constraint are respectively $(Ax)_i = b_i$ and $(Ax)_i = b_i + p_i$.

The hyperplane passing through the intersection of the hyperplanes

$cx = m + m'$ and $(Ax)_i = b_i$ is

$$cx + \lambda(Ax)_i - m - m' - \lambda b_i = 0 \qquad (3.1.1)$$

and that passing through the intersection of the hyperplanes

$cx = m$ and $(Ax)_i = b_i + p_i$ is

$$cx + \lambda'(Ax)_i - m - b_i + p_i = 0. \qquad (3.1.2)$$

It is easily seen that these two hyperplanes (3.1.1) and (3.1.2) become identical when $\lambda = \lambda' = m'/p_i$. Hence the hyperplane passing through both

$cx - m - m' = 0 = (Ax)_i - b_i$ and $cx - m = 0 = (Ax)_i - b_i - p_i$ is

$$p_i cx + m' (Ax)_i = p_i m + p_i m' + m'b_i . \qquad (3.1.3)$$

The hyperplane (3.1.3) may be called as the ith effective hyperplane. Noting the fact that the feasible region corresponding to the effective constraints must contain the original feasible region, the ith effective constraint is taken as

$$p_i cx + m' (Ax)_i \leq p_i m + p_i m' + m'b_i . \qquad (3.1.4)$$

3.2 Equivalent crisp LPP :

For each i = 1,2,....., m replacing the fuzzy constraint $(Ax)_i \lesssim b_i$ of the LPP (2.2) by the effective constraint (3.1.4) the equivalent crisp LPP of the fuzzy LPP (2.2) is obtained as

Maximize $z = cx$

subject to $p_i cx + m'(Ax)_i \leq p_i m + p_i m' + m'b_i$ $i = 1,2,....., m$ (3.2.1)

and $x \geq o$.

Comparing the crisp LPP (2.3) and (3.2.1) it is seen that the number of constraints in (2.3) is always more than the number of constraints in (3.2.1) by one. Also the number of variables in (2.3) is one more than that in (3.2.1). Hence in the simplex method the LPP (3.2.1) needs less computations that needed for the LPP (2.3).

4. NUMERICAL ILLUSTRATION

To illustrate the method two examples are considered one of which is due to Werners [4,5].

Example 4.1

Werners [4,5] considered the fuzzy LP model

$$\begin{aligned} \text{Maximize } z = \; & 2x_1 + x_2 \\ \text{subject to} \quad & x_1 \lesssim 3 \\ & x_1 + x_2 \lesssim 4 \\ & 0.5x_1 + x_2 \lesssim 3 \\ \text{and} \quad & x_1 , x_2 \geq 0 \end{aligned} \qquad (4.1.1)$$

with "tolerance intervales" of the fuzzy constraints as $p_1 = 6$, $p_2 = 4$, $p_3 = 2$.

To get m and m+m' we are to solve two crisp LP problems

$$\begin{aligned} &\text{Maximize } z = 2x_1 + x_2 \\ &\text{subject to } x_1 \le 3 \\ &\quad x_1 + x_2 \le 4 \\ &\quad 0.5x_1 + x_2 \le 3 \\ &\text{and } x_1, x_2 \ge 0 \end{aligned} \tag{4.1.2}$$

and

$$\begin{aligned} &\text{Maximize } z = 2x_1 + x_2 \\ &\text{subject to } x_1 \le 9 \\ &\quad x_1 + x_2 \le 8 \\ &\quad 0.5x_1 + x_2 \le 5 \\ &\text{and } x_1, x_2 \ge 0. \end{aligned} \tag{4.1.3}$$

The optimal solution of the LPP (4.1.2) is $x_1 = 3$, $x_2 = 1$, $z_{max} = 7$ and

that of the LPP (4.1.3) is $x_1 = 8$, $x_2 = 0$, $z_{max} = 16$.

$\therefore$ m = 7 and m + m' = 16 i.e. m = 7 and m' = 9.

Using Werners's method the equivalent crisp LPP is

$$\begin{aligned} &\text{Maximize } z = \alpha \\ &\text{subject to } 2x_1 + x_2 - 9\alpha \ge 7 \\ &\quad x_1 + 6\alpha \le 9 \\ &\quad x_1 + x_2 + 4\alpha \le 8 \\ &\quad 0.5x_1 + x_2 + 2\alpha \le 5 \\ &\text{and } x_1, x_2, \alpha \ge 0. \end{aligned} \tag{4.1.4}$$

This LPP contains 4 constrainsts in 3 variables and applying simplex method the optimal solution x_1 = 5.84, x_2 = 0.05 and α = 0.53 is obtained in 4 iterations (each table containing 8 columns).

Using the method of effective constriants the equivalent crisp LPP is

$$\begin{aligned} &\text{Maximize } z = 2x_1 + x_2 \\ &\text{subject to } 7x_1 + 2x_2 \le 41 \\ &\quad 17x_1 + 13x_2 \le 100 \\ &\quad 8.5x_1 + 11x_2 \le 59 \\ &\text{and } x_1, x_2 \ge 0 \end{aligned} \tag{4.1.5}$$

This LPP has 3 constriants in 2 variables and simplex method needs only 3 iterations (each containing only 5 columns to yield the optimal solution x_1 = 5.84, x_2 = 0.05, z_{max} = 11.737.

Example 4.2

In the standared form (2.2) of the fuzzy LPP with only fuzzy constraints 'b' is taken to be unrestricted in sign. To discuss this situation containing some components of 'b' positive and some negative the following LP model is considered.

$$\begin{aligned} \text{Maximize } z = \; & x_1 + x_2 - 2x_3 \\ & -8x_1 + 2x_2 - 3x_3 \lesssim -10 \\ & 2x_1 - 2x_2 + 3x_3 \lesssim 10 \\ & 2x_2 - x_3 \lesssim 4 \\ & x_1 - x_2 \lesssim 2 \\ & 5x_1 - 2x_2 + 3x_3 \lesssim 20 \\ & -x_1 - x_2 + x_3 \lesssim -5 \\ \text{and} \quad & x_1, x_2, x_3 \geq 0. \end{aligned} \tag{4.2.1}$$

The tolerance intervals of the fuzzy constraints are $p_1 = 2$, $p_2 = 5$, $p_3 = 3$, $p_4 = 10$, $p_5 = 6$ and $p_6 = 3$. Here it is easily seen that $m = 6$ and $m' = 8$.

The equivalent crisp LPP of the fussy LPP (4.2.1) in Werners's method is

$$\begin{aligned} \text{Maximize} \quad & z = \alpha \\ \text{subject to} \quad & x_1 + x_2 - 2x_3 - 8\alpha \geq 6 \\ & 8x_1 - 2x_2 + 3x_3 - 2\alpha \geq 8 \\ & 2x_1 - 2x_2 + 3x_3 + 5\alpha \leq 15 \\ & 2x_2 - x_3 + 3\alpha \leq 7 \\ & x_1 - x_2 + 10\alpha \leq 12 \\ & 5x_1 - 2x_2 + 3x_3 + 6\alpha \leq 26 \\ & x_1 + x_2 - x_3 - 3\alpha \geq 2 \\ & x_1, x_2, x_3, \alpha \geq 0. \end{aligned} \tag{4.2.2}$$

To solve the LPP (4.2.2) simplex method requires 6 tables each containing 14 columns. The optimal solution is $x_1 = 5.95$, $x_2 = 2.96$, $x_3 = 0$, $\alpha = 0.36$.

The equivalent crisp LPP obtained by the present method is

$$\begin{aligned} \text{Maximize } z = \; & x_1 + x_2 - 2x_3 \\ \text{subject to} \quad & 31x_1 - 9x_2 + 14x_3 \geq 26 \\ & 21x_1 - 11x_2 + 14x_3 \leq 150 \\ & 3x_1 + 19x_2 - 14x_3 \leq 74 \\ & 9x_1 + x_2 - 10x_3 \leq 78 \\ & 23x_1 - 5x_2 + 6x_3 \leq 122 \\ & -5x_1 - 5x_2 + 2x_3 \leq 2 \\ \text{and} \quad & x_1, x_2, x_3, \geq 0. \end{aligned} \tag{4.2.3}$$

The same solution $x_1 = 5.95, x_2 = 2.96, x_3 = 0$ and $z = 8.903$ is obtained here in only 4 tables of simplex method each table containing only 10 columns.

ACKNOWLEDGEMENTS:

The authors thank the referee for his valuable comments and suggestions to improve the paper.

References :

1. **Bellman, R. and Zadeh, L.A.** Decision making in a fuzzy environment, *Management Science 17 (1970)B141-164.*
2. **Werners, B.** Interactive multiple objective programming subject to feasible constraints. *European Journal of Operational Research 31(1987) 342-349.*
3. **Werners, B.**, An interactive fuzzy programming system. *Fuzzy Sets and Systems 23(1987) 131-137.*
4. **Werners, B.,** Interaktive Entscheidungs unterstutzung durch ein flexibles mathematischees Programmierungs system. *Munchen (1984).*
5. **Lai, Y. J. and Hwang, Ch.L.** Fuzzy Mathematical Programming, Methods and Applications. *Springer–Verlag.*

Hall Effects on Hydromagnetic Flow in a Horizontal Channel in the Presence of Inclined Magnetic Field

G. Dogra, A. K. Kanch and R. N. Jana

Department of Applied Mathematics, Vidyasagar University
Midnapore - 721 102, West Bengal, India.

Hall effects on the hydromagnetic flow of a viscous incompressible conducting fluid between two horizontal perfectly conducting plates in the presence of a uniform magnetic field which is inclined with the positive direction of vertical axis is considered. It is found that the primary velocity increases while the secondary velocity decreases with increase in angle of inclination of the applied magnetic field. It is also found that for large Hartmann number, there exists a thin boundary layer near the plates. The thickness of this layer increases with increase in angle of inclination of the magnetic field.

1. INTRODUCTION

It is well known (see cowling [1]) that the Hall currents become important when the strength of the magnetic field is very strong. Hall effects on the hydromagnetic flow of a viscous incomperssible liquid through parallel plates channel have been studied by Sato [2], Yamanishi [3], Sherman and Sutton [4]. In all these studies they have considered the transverse applied magnetic field. The present investigation, is developed to the study of the effects of Hall current on flow when the applied magnetic field is inclined at an angle θ with the positive direction of the vertical axis. An exact solution of the governing equation of the fully developed flow is obtained. It is found that for large values of Hartmann number, there exists a thin boundary layer near the plates which increases with increase in angle of inclination (θ) of the applied magnetic field. It is also found that the boundary layer thickness is independent of the Hall parameter m.

2. Mathematical formulation and its solution

Consider the fully developed steady flow of an electrically conducting viscous incompressible fluid between two infinite long perfectly conducting plates separeted by a distance 2 L. The origin of the cartesian coordinate system is taken at the central region of the channel, x-axis in the direction of flow and z-axis perpendicular to it. A uniform magnetic field H_0 is applied along z-axis which is inclimed at an angle θ with the positive direction of z-axis. For fully deveoped flow all physical quantities, except pressure, will be function of z-only. Since Hall currents interacts with the magnetic field to generate a transverse motion of the fluid, the flow and the magnetic field can be taken as (u, v, o) and ($H_x + H_o \sin\theta, H_y, H_o \cos\theta$) respectively. The equations of momentum and the magnetic induction equations, taking Hall current into account, can be written as

$$0 = -\frac{\partial p}{\partial x} + \mu \frac{d^2u}{dz^2} + \mu_e H_o \cos\theta \frac{dH_x}{dz} \qquad (1)$$

$$0 = \mu \frac{d^2v}{dz^2} + \mu_e H_o \cos\theta \frac{dH_Y}{dz} \tag{2}$$

$$0 = -\frac{\partial p}{\partial z} - H_Y \frac{dH_Y}{dz} - (H_X + H_o \cos\theta) \frac{dH_X}{dz} \tag{3}$$

$$-\frac{d^2H_X}{dz^2} - \omega_e \tau_e \frac{d^2H_Y}{dz^2} = \sigma \mu_e H_o \cos\theta \frac{du}{dz} \tag{4}$$

$$-\frac{d^2H_Y}{dz^2} + \omega_e \tau_e \frac{d^2H_X}{dz^2} = \sigma \mu_e H_o \cos\theta \frac{dv}{dz} \tag{5}$$

where μ is the coefficient of viscosity, μ_e the magnetic permeability, ρ the fluid density, σ the fluid conductivity, ω_e the cyclotron frequency and τ_e the elctron collision time.

The boundary conditions for the velocity and the magnetic fields are respectively

$$u = v = 0 \quad \text{at} \quad y = \pm L$$

$$\frac{dH_X}{dz} = \frac{dH_Y}{dz} = 0 \text{ at } y \pm L. \tag{6}$$

Introducing non-dimensional variables

$$\eta = y/L,\ u_1 = uL/\nu,\ v_1 = vL/\nu,\ h_x = H_x/\sigma \mu_e \nu H_o,$$

$$h_y = H_Y/\sigma \mu_e \nu H_o, \tag{7}$$

equations (1), (2), (4) and (6) beccome

$$\frac{d^2u_1}{d\eta^2} + M^2 \cos\theta \frac{dH_X}{d\eta} = -R \tag{8}$$

$$\frac{d^2v_1}{d\eta^2} + M^2 \cos\theta \frac{dh_Y}{d\eta} = 0 \tag{9}$$

$$\frac{d^2h_X}{d\eta^2} + m \cos\theta \frac{d^2h_Y}{d\eta^2} + \cos\theta \frac{du_1}{d\eta} = 0, \tag{10}$$

$$\frac{d^2h_Y}{d\eta^2} - m \cos\theta \frac{d^2h_X}{d\eta^2} + \cos\theta \frac{dv_1}{d\eta} = 0, \tag{11}$$

where $M = \left(\sigma \mu_e^2 H_o^2 L^2/\rho\nu \right)^{1/2}$, the Hartmann number, $m = \omega_e \tau_e$ the

Hall parameter and $R = \frac{L^3}{\rho\nu} \left(-\frac{\partial p}{\partial x} \right)$ the non-dimensional pressure gradient.

The boundary conditions (6) become

$$u_1 = v_1 = 0 \quad \text{and} \quad \frac{dh_x}{d\eta} = \frac{dh_y}{d\eta} = 0 \text{ at } \eta = \pm 1. \tag{12}$$

The solution of the equations (8) – (11) subject to the boundary conditons (12) are

$$F(\eta) = \frac{R(\alpha - i\beta)^2}{(\alpha^2+\beta^2)^2} \left[1 - \frac{\cosh(\alpha + i\beta)\eta}{\cosh(\alpha + i\beta)} \right], \tag{13}$$

$$h(\eta) = \frac{R\cos\theta\,(\alpha - i\beta)^2\,(1 + im\cos\theta)}{(\alpha^2 + \beta^2)\,(1 + m^2\cos^2\theta)} \left[\frac{\sinh(\alpha + i\beta)\eta}{(\alpha+i\beta)\cosh(\alpha+i\beta)} - \eta \right], \tag{14}$$

where

$$F(\eta) = u_1 + iv_1 \text{ and } h(\eta) = h_x + ih_y \tag{15}$$

$$\alpha = \frac{1}{\sqrt{2}} \left[\frac{M^2\cos^2\theta}{1 + m^2\cos^2\theta} \left\{ \left(1 + m^2\cos^2\theta \right)^{1/2} + 1 \right\} \right]^{1/2}$$

$$\beta = \frac{1}{\sqrt{2}} \left[\frac{M^2\cos^2\theta}{1 + m^2\cos^2\theta} \left\{ \left(1 + m^2\cos^2\theta \right)^{1/2} - 1 \right\} \right]^{1/2} \tag{16}$$

On separating real and imaginary parts, we can readily find x and y-components of velocity and magnetic field from equations (13) and (14).

We now discuss a few particular cases of interest.

Case – I : When $M^2 << 1$ and $m^2 << 1$.

Neglecting square and higher powers of M^2 and m^2 in (13) and (14) and on using (15), we get

$$\frac{u_1}{R} = \frac{1}{2}\left(1 - \eta^2\right) + M^2\cos^2\theta \left(-\frac{5}{24} + \frac{1}{4}\eta^2 - \frac{1}{24}\eta^4 \right) + \text{-------} \tag{17}$$

$$\frac{v_1}{R} = m\,M^2\cos^2\theta \left(-\frac{5}{24} + \frac{1}{4}\eta^2 - \frac{1}{24}\eta^4 \right) + \text{-------}, \tag{18}$$

$$\frac{h_x}{R} = \cos\theta \left[\left(\frac{1}{3}\eta^3 - \frac{1}{2}\eta \right) + \frac{M^2\cos^2\theta}{12} \left(\frac{1}{10}\eta^5 - \eta^3 + \frac{5}{2}\eta \right) + \text{----} \right], \tag{19}$$

$$\frac{h_y}{R} = m\cos^2\theta \left[\left(\frac{1}{3}\eta^3 - \frac{1}{2}\eta \right) + \frac{1}{6}M^2\cos^2\theta \left(\frac{1}{10}\eta^6 - \eta^3 + \tfrac{5}{2}\eta \right) + \text{----} \right]. \tag{20}$$

The above expressions show that for weak applied magnetic field, the velocity and the magnetic field in the x-direction is independent of Hall parameter m. It is seen that in the absence of magnetic field, the problem is reduced to the classical hydrodynamic flow through a straight channel under constant pressure gradient and we have.

$$u_1 = \frac{R}{2}(1-\eta^2), \quad v_1 = 0. \tag{21}$$

Case - II. When $M^2 >> 1$ and $m^2 << 1$.

When M^2 is large and m is small in order of magnitude, the boundary layer type flow is expected. Writing $\zeta = 1-\eta$, we get

$$u_1 = \frac{R}{M^2\cos^2\theta}\left(1 - e^{-M\zeta\cos\theta}\right), \tag{22}$$

$$v_1 = \frac{R}{M^2\cos^2\theta}\left[-m\cos\theta\left(1-e^{-M\zeta\cos\theta}\right) + \tfrac{1}{2}M\,m\cos^2\theta\,\zeta\,e^{-M\zeta\cos\theta}\right], \tag{23}$$

$$h_x = \frac{R}{M^2\cos\theta}\left[\zeta + \frac{1}{M\cos\theta}e^{-M\zeta\cos\theta}\right]. \tag{24}$$

$$h_y = \frac{mR}{M^2}\left[\frac{1}{2}\zeta e^{-M\zeta\cos\theta} + e^{-M\zeta\cos\theta}\right]. \tag{25}$$

The above equations (22) and (23) show the existance of a thin boundary layer of order $O(1/M\cos\theta)$ in the vicinity of the plates. It is seen that the thickness of the boundary layer is independent of Hall parameter m. It is also seen that the thickness of the boundary layer increases with increase in θ and becomes infinite when $\theta = 90^\circ$. The expression (22) and (24) show that both the velocity and the magnetic field in the x-direction are independent of Hall parameter m. In the central core given by $\zeta \geq 1/M\cos\theta$ about the vertical axis of the channel, the velocity and the magnetic field become

$$u_1 = R/M^2\cos^2\theta, \qquad v_1 = -mR/M^2\cos^2\theta, \tag{26}$$

$$h_x = \frac{R}{M^2\cos\theta}\zeta, \quad h_y = 0. \tag{27}$$

It is evident from the above equations (26) and (27) that in the central region the secondary velocity is weak in comparision to the primary flow and the induced megnetic field $h_y = 0$.

3. Results and Discussions

The primary and secondary velocity profiles have been plotted against η for farious values of M^2, θ and m in figures 1 and 2 respectively. It is seen that for fixed values of M^2 and m, the primary velocity increases while secondary velocity decreases with increase in θ. It is also seen that both the primary and secondary velocity increase with increase in Hall parameter m when M^2 and θ are fixed. Further, for fixed values of m and θ,at any point both are velocity components decrease with increase in M^2, as expected, since the magnetic field exerts a retarding influence on the flow.
We have presented the non-dimensional magnetic field components h_x and h_y against η for $M^2 = 5$ and for dirrerent values of θ and m in figure 3. It is seen that both h_x and h_y decrease with increase in m for fixed values of θ and M^2. It is also seen that for fixed values of M^2 and m, both h_x and h_y increase for $h_x \leq 45^o$ and decrease for $\theta > 45^o$.

The non-dimensional shear - stress due to primary and the secondary flow at the plate $\eta = \pm 1$ are respectively.

$$\tau_x = \left(\frac{du_1}{d\eta}\right) \eta = \pm 1 = \pm \frac{R(\alpha \sinh 2\alpha - \beta \sin 2\beta)}{(\alpha^2+\beta^2)(\cosh 2\beta + \cos 2\beta)}, \tag{28}$$

and

$$\tau_y = \left(\frac{dv_1}{d\eta}\right) \eta = \pm 1 = \pm \frac{R(\beta \sinh 2\alpha - \alpha \sin 2\beta)}{(\alpha^2+\beta^2)(\cosh 2\alpha + \cos 2\beta)}, \tag{29}$$

The non-demensional shear stresses τ_x and τ_y at the plate $\eta = 1$ have been plotted against Hall parameter m for various values of θ and for $M^2 = 10$ in figure 4. It is observed that both τ_x and τ_x increase with increase in either m or θ. On using (16), it is found form (28) and (29) that in the absence of Hall currents ($m = 0$), the non-dimensional shear stress at plate $\eta = 1$ in the x and y - directions are respectively.

$$\tau_x = \pm \frac{\tanh(M \cos\theta)}{M \cos\theta} \quad \text{and} \quad \tau_y = 0. \tag{30}$$

Above relations show that in the absence of Hall current ($m = 0$), the shear stress due to secondary flow vanishes, as expected, at both the plates while that due to the primary flow vanishes neither at the upper plate ($\eta = 1$) nor at the lower ($\eta = -1$)

References :

1. **T. G. Cowling ,** Magnetohydrodynamics Interscience, New York, 1957, **101**
2. **H. J. Sato,** *J. Phys. Soc. Japan* **16** (1961), **1427**
3. **T. Yamanishi,** Preprint, 17th Annual Meeting, *Phys. Soc.*Japan, Osaka, **5**(1962), **29**
4. **A. Sherman, W. Sutton,** Engineering Magnetohydrodynamics, Mc-Graw Hill, New York, (1965) **363**

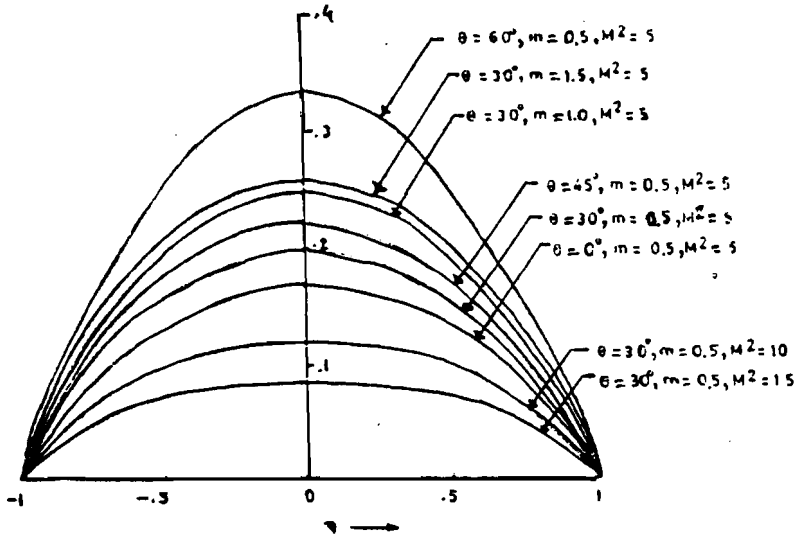

Fig. 1 Velocity u_1

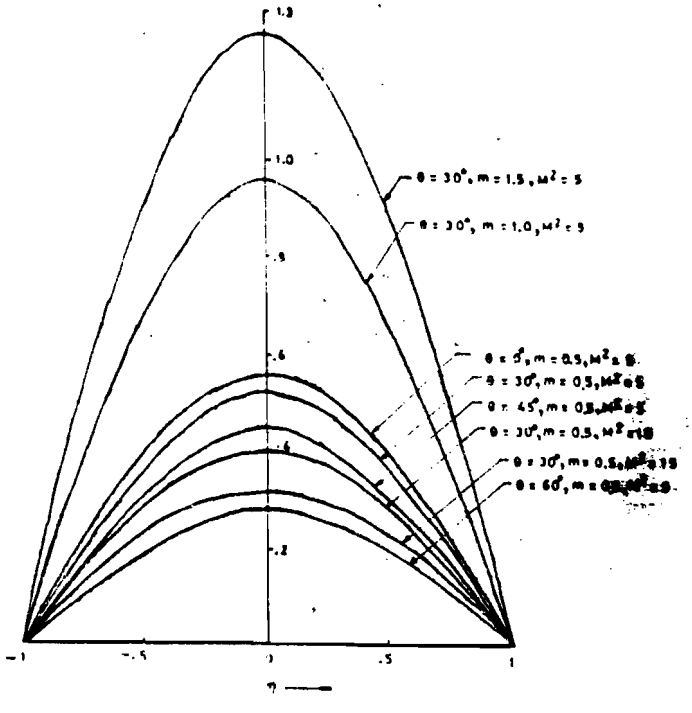

Fig. 2 Velocity v_1

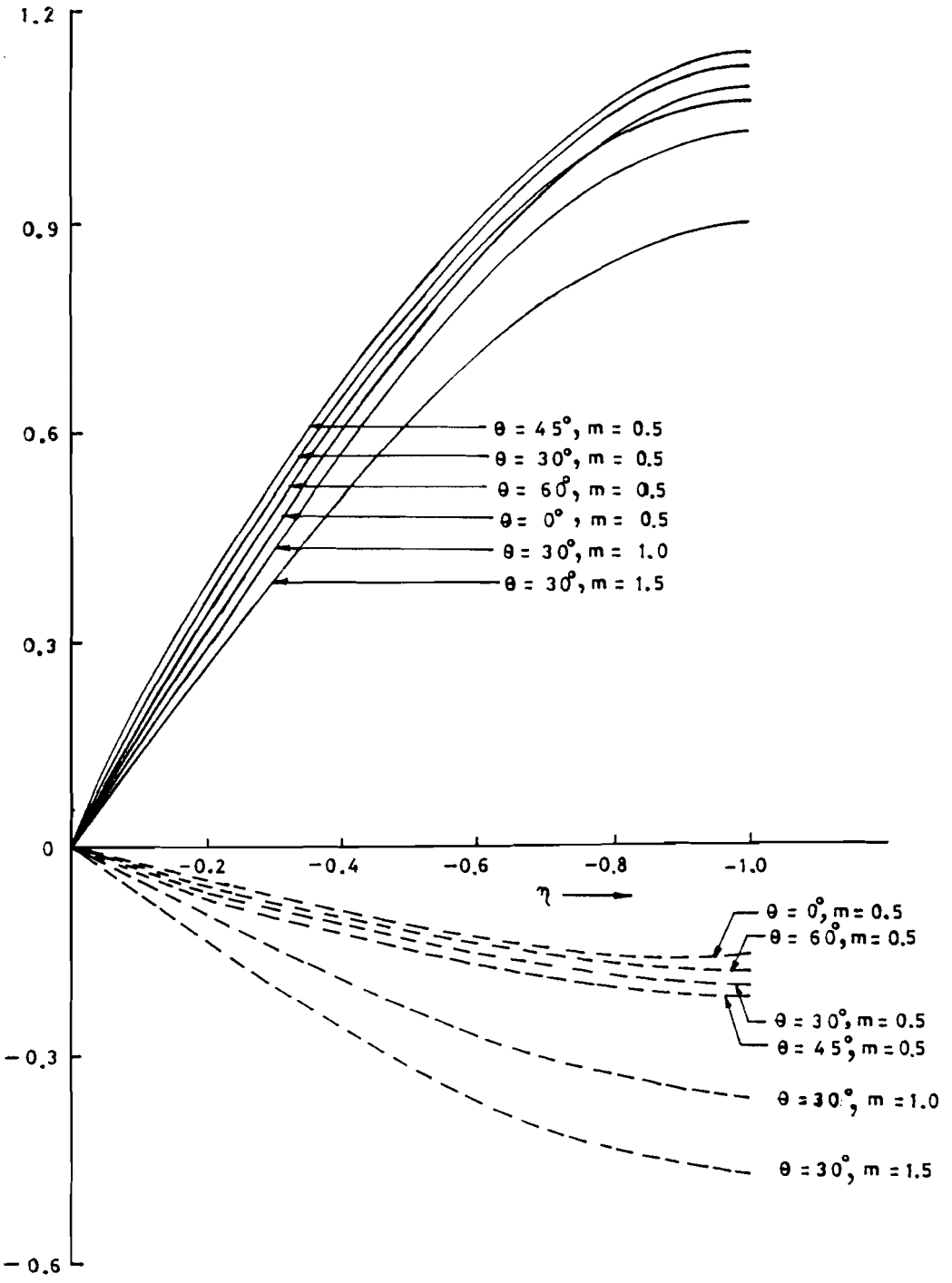

Fig. 3 ——$10 \times h_x$, ------ $10 \times h_y$ for $M^2 = 5.0$

On a Type of Semi-Symmetric Metric Connection on a Riemannian Manifold

U. C. De And B. K. De

Department of Mathematics, University of Kalyani, Kalyani, - 741 235, West Bengal, India.

Key words : Semi-symmetric metric connection, Weyl conformal curvature tensor, conformally flat manifold.

1. INTRODUCTION:

Fridemann and Schouten [a] introduced semi-symmetric connection. Yano [b] synthesized the notion of semi-symmetric connection. He also proves that a Riemannian manifold admits a semi-symmetric metric connection of zero curvature tensor if and only if it is conformally flat [b]. The object of this paper is to study a Riemannian manifold which admits a semi-symmetric metric connection with a certain form of curvature tensor.

Consider an n-dimensional orientable Riemannian manifold with a metric tensor g and its Levi-civita connection ∇. We consider all geometric objects on M be sufficiently smooth. Denote arbitrary vector fields on M by X,Y and Z etc. A linear connection $\bar{\nabla}$ on M is said to be a semi-symmetric metric connection [b] if there exists a 1-form π such that the torsion tensor T is given by

$$T(X,Y) = \pi(Y)X - \pi(X)Y \tag{1}$$

and $\bar{\nabla} g = 0$

For such a metric connectionn [b]

$$\bar{\nabla}_X Y = \nabla_X Y + \pi(Y)\, X - g(X,Y)\, P \tag{2}$$

where P is a vector field such that $g(P,X) = \pi(X)$. We denote the curvature tensor, Ricci tensor of type (0,2), the scalar curvature and the Weyl conformal curvature tensor of M with respect to ∇ by R, S, r, C respectively. A bar over them refers to $\bar{\nabla}$. We know that [b]

$$\bar{R}(X,Y)Z = R(X,Y)Z - \alpha(Y,Z)X + \alpha(X,Z)\, Y$$

$$- g(Y,Z)\, AX + g(X,Z)\, AY \tag{3}$$

where

$$\alpha(X,Y) = (\nabla_X \pi)(Y) - \pi(X)\, \pi(Y) + \tfrac{1}{2}\, \pi(P)\, g(X,Y) \tag{4}$$

and

$$AX = \nabla_X P - \pi(X)P + \tfrac{1}{2}\, \pi(P)X \tag{5}$$

In this connection we recall that

$$S(X,Y) = \sum_{i=1}^{n} R(X,V_i,V_iY)$$

where $\{V_i\}$ is an orthonormal basis of the tangent space at each point of the manifold M.

$$C(X,Y)Z = R(X,Y)Z + \lambda(Y,Z)X - \lambda(X,Z)Y + g(Y,Z)LX - g(X,Z)LY, \quad (6)$$

where $\lambda(X,Y) = -\frac{1}{(n-2)} S(X,Y) + \frac{r}{2(n-1)(n-2)} g(X,Y)$ (7)

and $g(LX,Y) = \lambda(X,Y)$

1. In this section we deal with the implications of the prescription

$$\bar{R}(X,Y)Z = \phi R(X,Y)Z,$$

where ϕ is a real function on M.

Lemma 1. If $\bar{R}(X,Y)Z = \phi R(X,Y)Z$, ϕ a real function on M, then

$$(1-\phi) S(X,Y) = (n-2)\,\alpha(X,Y) + a\,g(X,Y) \quad (1.1)$$

$$(1-\phi)r = 2(n-1)\,\mathrm{div}\,P + (n-1)(n-2)\,\pi(P) \quad (1.2)$$

$$\alpha(X,Y) = (\phi - 1)\,\lambda(X,Y) \quad (1.3)$$

where a is the trace of A and n>3.

Proof. From (3) we can write

$$g[\bar{R}(X,Y)Z, W] = g[R(X,Y)Z,W] - g[\alpha(Y,Z)X,W] + g[\alpha(X,Z)Y,W] - g[g(Y,Z)AX,W] + g[g(X,Z)AY,W] \quad (1.4)$$

Putting X = W in (1.4) and from the given hypothesis we have

$$\phi\, g[R(X,Y)Z, X] = g[R(X,Y)Z,X] - g[\alpha(Y,Z)X,X] + g[\alpha(X,Z)Y,X] - g[g(Y,Z)AX,X] + g[g(X,Z)AY,X] \quad (1.5)$$

Let us take $X = V_i$, then (1.5) becomes

$$\phi\, g[R(V_i,Y)Z, V_i] = g[R(V_i,Y)Z,V_i] - g[\alpha(Y,Z)V_i,V_i] + g[\alpha(V_i,Z)Y,V_i] - g[g(Y,Z)AV_i,V_i] + g[g(V_i,Z)AY,V_i] \quad (1.6)$$

From (1.6) we get

$$\phi S(Y,Z) = S(Y,Z) - n\,\alpha(Y,Z) + 2\,\alpha(Y,Z) - ag(Y,Z)$$

i.e., $$(1-\phi)\,S(Y,Z) = (n-2)\,\alpha(Y,Z) + ag(Y,Z) \tag{1.7}$$

This completes the proof of (1.1)

Using the relation (4) and (5) we get from (1.7)

$$(1-\phi)\,S(X,Y) = (n-2)\,[\,g(\,Y,\,\nabla_X P) - g(X,P)\,g(Y,P) + \tfrac{1}{2}\,g(P,P)\,g(X,Y)] + (\mathrm{div}P - \frac{n-2}{2}\pi(P))\,g(X,Y) \tag{1.8}$$

Putting $X = Y = V_i$ in (1.8) we get

$$(1-\phi)r = 2(n-1)\,\mathrm{div}P + (n-1)\,(n-2)\,\pi(P)$$

This completes the proof of (1.2)

Putting $X = Y = V_i$ in (1.1) gives

$$(1-\phi)\,r = (n-2)\,a + a\,n \tag{1.9}$$

where a is the trace of A.

Using (1.1) and (1.9) in (7) we get

$$\lambda(X,Y) = -\frac{1}{n-2}\,[\,\frac{1}{1-\phi}\,\{(n-2)\,\alpha(X,Y) + a\,g\,(X,Y)\}\,] + \frac{\frac{1}{1-\phi}\,\{(n-2)a + a\,n\}}{2(n-1)\,(n-2)}\,g\,(X,Y) \tag{1.10}$$

Now from (1.10) we have

$$\alpha(X,Y) = (\phi - 1)\,\lambda(X,Y)$$

This completes the proof of (1.3)

Now using (1.3) in (3) we get

$$\begin{aligned}\bar{R}\,(X,Y)Z &= R(X,Y)Z - (\phi-1)\,\lambda(Y,Z)X - (\phi-1)\,\lambda(X,Z)Y \\ &\quad - g(Y,Z)\,AX + g(X,Z)\,AY \\ &= R(X,Y)Z + \phi R(X,Y)Z - \phi R(X,Y)\,Z - \phi\,\lambda(Y,Z)X \\ &\quad + \lambda(Y,Z)\,X + \phi\,\lambda(X,Z)Y - \lambda(X,Z)Y - g(Y,Z)AX + g(X,Z)AY \end{aligned} \tag{1.11}$$

Now $g(g(Y,Z)AX,W) = g(Y,Z)\, g(AX,W)$

$= g(Y,Z)\, \alpha(Z,W)$

$= g(Y,Z)\, (\phi - 1)\, \lambda(X,W)$, [from (1.3)]

$= (\phi - 1)\, g(Y,Z)\, g(LX,W)$

$= g((\phi - 1)\, g(Y,Z)\, LX, W$

$\therefore\ g(Y,Z)\, AX = (\phi - 1)\, g(Y,Z)\, LX$ (1.12)

Similarly $g(X,Z)\, AY = (\phi - 1)\, g(X,Z) LY$ (13)

Using (1.12) and (1.13) in (1.11) it follows that

$$(\phi - 1)\, C(X,Y)Z = 0$$

Thus we can state the following theorem :

Theorem If a Riemannian manifold M of demension $n > 3$ admits a semi-symmetric metric conrection such that $\bar{R} = \phi R$, ϕ is a real function on M, then the following relation holds

$$(1 - \phi)\, C(X,Y)Z = 0$$

If $\phi = 0$, then from the above theorem we can state the following corollary.

Corollary If a Riemannian manifold admits a semi-symmetric metric connection whose curvature tensor vanishes, then the maniflod is contormally flat.

The above corollary has been proved by K. Yano [b] in another way.

References :

1. **A. Friedmann, and J. A. Schouten, :** Uber die Geometric der helbsymmetrischen Uber tragungen, *Math.* **21** (1924), **211-223.**
2. **K. Yano, :** On semi-symmetric metric connection, Rev. Roum. *Math.* Pures *et* Appl., **15** (1970), **1579-1581.**

Evaluation of second exponential integral and its applications to thermal analysis

W.G. Devi
Chemistry Department, T.S. Paul Manipur Women's College
Mongsangei, Imphal-795008, Manipur

Abstract : In the present paper a precise method for evalution of second exponential integral is presented. The suitability of the method is tested by evaluating an untegral which frequently occurs in thermal analysis problems. The method has also been checked by fitting experimental differential thermal analysis curves.

Key Words : Second exponential integral, differential thermal analysis, activation energy, order of kinetics, pre-exponential factor.

1. INTRODUCTION :

Nonisothermal thermoanalytical techniques are widely used in the analysis of different types of reactions such as chemical reactions and diffusion controlled reactions etc. Nonisothermal analysis of reactions normally involve the heating of reactants from ambient temperature to high temperature to enable reactants to undergo some transformation. By means of such analysis a group of phenomena namely thermogravimetry (TG), differential thermal analysis (DTA) and differential scanning calorimetry (DSC) can be studied. Mathematical modelling of these processes leads of their fuller understanding thereby checking the validity of assumptions and deducting quantitative conclusions from apparent kinetic parameters. These techniques [1-3] have been widely used for identification of many types of materials, the study of properties like thermal stability and the investigation of various processes of practical importance. But a major limitation of mathematical modelling non-isothermal techniques arises due to complication in the mathematical analysis of the data due to the fact that the integral $\int_0^T \exp(-E/RT')dT'$ (E=activation energy, R=universal gas constant, T the temperature in Kelvin occuring in the analysis has no closed from solution. This integral can be written in terms of the second exponential[4] $E_2(u)$. In the present article a method of evaluation of second exponential integral is presented. The accuracy of the present method is tested by evaluating the integral $\int_0^T \exp(-E/RT')dt'$ for various values of u=E/RT and comparing with the results of a recent paper by Quanyin and Su[5]. Finally a further check of present method is done by fitting experimental DTA curves[6,7] of the dehydration of $Ni[mpipz)_2(NCS)_2]$ and decomposition of $Ca(DMP)_2(MCA)_2$, where mpipz, DMP and MCA respectively stand for N-methyipiperazine, dimethyipiperazine and monochloroacetato.

2. Theory

The second exponential integral is defined as[4]

$$E_2(u)=\int_0^\infty (1/t^2)\exp(-ut)dt \qquad (1)$$

A continued fraction development for $E_2(u)$ is given by [8]

$$E_2(u)=\exp(-u)\left(\frac{1}{u+}\ \frac{2}{1+}\ \frac{1}{u+}\ \frac{3}{1+}\ \frac{2}{u+}\ \cdots\cdots\right) \qquad (2)$$

where $a_1 + \cfrac{b_1}{a_2 + \cfrac{b_2}{a_3 + \cdots}}$ ..... is the compact form of the continued fraction[9]

$$a_1 + \cfrac{b_1}{a_2 + \cfrac{b_2}{a_3 + \cdots}}$$

The present method has the advantage that it convergres rapidly for u>1 and is highly precise. For u<1, $E_2(u)$ is evaluated by using the expression

$$E_2(u) = \exp(-u) - u\ln u - \sum_{R=0}^{5} a_k u^k \qquad (3)$$

where the coefficients a_k's are given by

$a_0 = 0.57721566$

$a_1 = 0.99999193$

$a_2 = -0.24991055$

$a_3 = 0.05519968$

$a_4 = -0.00976004$

$a_5 = 0.00107857$

Now the integral $\int \exp(-E/RT')dT'$ occuring in the mathematical modelling of the non-isothermal thermal analysis can be expressed as

$$\begin{aligned} I(T) &= \int_0^T \exp(-E/RT')\,dT' \\ &= (E/R)\int_0^\infty \exp(-u')/u'^2 du' \quad (\text{with } u' = E/RT') \\ &= (E/R)\int_0^\infty \exp(-tu)/t^2 dtu \quad (u' = tu) \\ &(E/Ru)E_2(u) \quad (\text{from (1)}) \end{aligned} \qquad (4)$$

3. Results and discussions

The values of the second exponential integral computed by the present technique are in excellent agreement with those reported in Abramowitz and Stegun[4]. All computations have been carried out by using double precission arithmatic. For a further check of the present method the values of the integral $\int_0^T \exp(-E/RT')\,dT'$ evaluated by using the second exponential integral have been compared (Table 1) with the values of the integral evaluated numerically. The numerical evaluation have been carried out by using 32 point Gauss Legendre Quadrature method[4,10]. The range (0,T) have been divided into suitable number of subintervals. We see that the values of the integral computed by using the present method of the evaluation of the second exponential integral for all practical purposes are identical with those of numerical evaluation for all values of u. On the other hand it is evident from Table 1 that the method never completely agrees with the numerical result. Actually Quanyin and Su method fails for u<5.

Further in order to check the validity of the present technique an attempt has been made to fit the

experimental DTA curves of the dehydration reaction $Ni[(mpipz)_2(NCS)_2].2H_2O \rightarrow Ni[(mpipz)_2(NCS)_2$ and the decomposition reaction $Cd[(DMP)_2(MCA)_2] \rightarrow Cd[(DMP)(MCA)_2]$. Following Luo[11] for a DTA curve the expression for the temperature deviation ΔT from the horizontal baseline is given by

$$\Delta T = A\exp(-E/RT)\,[1+(n-1)(A/\phi)\int_{T_0}^{T}\exp(-E/RT')dT']^{-n/(n-1)} \qquad (n\neq 1) \qquad (5)$$

$$\Delta T = A\exp(-E/RT)\exp[-(A/\phi)\int_{0}^{T}\exp(-E/RT')dT'] \qquad (n=1) \qquad (6)$$

where A, the pre-exponential factor, n, the order of kinetics, ϕ, thelinear heating rate, T_0 the starting tempertaure and T, and temperature at time t. At the peak temperature $T=T_m$, the deflection of DTA curve is maximum so that

$$[d\Delta T/dT]_{T=Tm} = 0 \qquad (7)$$

From equations (6) and (7) one can write for n=1

$$\phi E/RT_m^2 = A\exp(-E/RT_m) \qquad (8)$$

Similarly for $n\neq 1$one gets

$$1+(n-1)((A/\phi)\int_{T_0}^{T}\exp(-E/RT')dT' = (nART_{m}^2/\phi E)\exp(-E/RT_m) \qquad (9)$$

The integral occuring in equations (5), (6) and (9) can be expressed in terms of the second exponential integral $E_2(u)$ (Equation (4)). It is chosen to define by $\Delta\bar{T}$, the experomental DTA results given in a graphical form from which one can use a certain number of points $\Delta\bar{T}_i$ for i=1,2,....N. The process is initiated with the arbitrary values of E and n. The pre-exponential factor A can be computed either from equation (8) (n=1) of from equation (9) ($n\neq 1$) using the present values of T_m, E, T_0 and n. The theoretical curve ΔT_i is computed from equation (5) ($n\neq 1$) or from (6) (n=1) and the mean deviation S_1 and root mean square deviation S_2 are calculated as

$$S_1 = (1/N)\Sigma[\Delta T_i - \Delta\bar{T}_i] \qquad (10)$$

$$S_2 = \{(1/N)\Sigma[\Delta T_i - \Delta\bar{T}_i]^2\}^{1/2} \qquad (11)$$

$S_1 = S_2 = 0$ will mean a complete coincidence of the theoretical and experimental DTA curves. An attempt has been made to find out the values of E and n, that minimize S_1 and S_2. For a given value of n, S_1 increases for decrease in values of E and vice versa. If S_1 is positive E is increased by adding a certain amount ΔE to it. The process is repeated until S_1 changes sign. Now half of the previous amount namely $0.5\Delta E$ is subtracted from E and this process is repeated, namely the correction is halved in each step and its sign is determined by the sign of S_1. Since S_1 is the sum of positive and negative differences it's absolute value can be reduced to any desired extent by changing E, independent of the value of n. Thus the process might be continued down to an arbitrarily small absolute value of S_1 until the chage in E is small enough. The dependence on the order of kinetics n has been checked by S_2. The value of n has been varied in small steps in order to reduce S_2 and in each step E is recalculated such that S_1 gets arbitrarily small. n is changed in acertain direction as long as S_2 decreases. If S_2 increases the direction of the change in n is altered. The process is terminated when the change in n is small enough. This method is applied to obtain the kinetic parameters E,A and n of the DTA peaks corresponding to the chemical reactions mentioned above (Table 2). The values of activation energies so determined are in fair agreement with those obtained[6,7] by using Borchardt and Daniels[12] method.

4. Conclusions

In the present paper a numerical technique has been developed for the computation of the second

exponential integral $E_2(u)$ for any $u>0$. The suitability of the present method has been assessed by the evaluation of the integral $\int_0^T \exp(-E/RT')\,dT'$ required in the analysis of the TG and DTA data. The technique has been tested further by developing a computer code for curve fitting and applying it to analyse some experimental DTA curves.

Acknowledgement

The author is grateful to Prof. Ak. Manlhar Singh and Dr. P. S. Mazumdar for their constant encouragement in the course of this work.

References :

1. **R. C. Mackenzie.,** *"Differential Thermal Analysis"*, Academic Press, London (1972).
2. **D. S. Bhunia., and S. K. Biswas,** Vidyasagar University *J. Physical Sciences,* **Vol. 1,** Chemistry Section, **P 4** (1995).
3. **N. K. De., C. Sinha, and P. Chattopadhyay,** Vidyasagar University *J. Physical Sciences,* **Vol. 1,** Chemistry Section, **P 8** (1995).
4. **M. Abramowitz. and I. A. Stegun.,** *"Handbook of Mathematical Functions"*, Dover Publications, New York, ch. 5 (1965).
5. **R. Quanyin., and Y. Su.,** *J. Thermal Anal.*, **Vol. 44, P 1147** (1995).
6. **L. K. Singh., and S. Mitra.,** *J. Chem.* Soc. Dalton Trans. **P 2089** (1987).
7. **R. K. B. Singh., and Mitra. S.,** *"Abstracts of 4rth Manipur Science Congress"*,Manipur University, India, **P 8** (1992).
8. **A. Erdelyi.,** *"Higher Transcendental Functions"* **Vol. 2,** McGraw-Hill, New York, ch. 9 (1953).
9. **H. S. Hall, and S. R. Knight,** "*Higher Algebra*" SBD Publishers, New Delhi (1995).
10. **D. T. Y. Chen., and P. H. Fong.,** Thermochil Acta, **Vol. 18 , P 170** (1977).
11. **K. M. Luo.,** Thermochim Acta, **Vol. 255, P 241** (1995).
12. **H. J. Borchardt. and F. Daniels.,** *J. Am Chem. Soc.*, **Vol. 79, P 41 (1957).**

Table 1. Values of the integral $\int_0^T$ exp(–E/RT') dT'

u=E/RT	Values of the integral $\int_0^T$ exp (–E/RT') dT'		
	Numerical	Present	Quanyin and Su[6]
0.5	326.6439	326.6439	63321.801
1	148.4955	148.4955	1324.366
2	37.5343	37.5343	0.0
3	10.6419	10.6419	2.7045
4	3.1982	3.1982	1.6312
5	9.9647(–1)*	9.9647(–1)	6.5978(–1)
6	3.1826(–1)	3.1826(–1)	2.4022(–1)
7	1.0351(–1)	1.0351(–1)	8.4313(–2)
8	3.4138(–2)	3.4138(–2)	2.9189(–2)
9	1.1384(–2)	1.1384(–2)	1.0059(–2)
10	3.8302(–3)	3.8302(–3)	3.4649(–3)
15	1.8108(–5)	1.8108(–5)	1.7313(–5)
20	9.4048(–8)	9.4048(–8)	9.1685(–8)
25	5.1569(–10)	5.1569(–10)	5.0731(–10)
30	2.3437(–12)	2.3437(–12)	2.3171(–12)
40	6.0757(–17)	6.0757(–17)	6.0365(–17)
50	1.8559(–21)	1.8559(–21)	1.8482(–21)
60	5.6522(–26)	5.6522(–26)	5.6359(–26)
70	2.7618(–30)	2.7618(–30)	2.7559(–30)

*A(–B) donotes $Ax10^{-B}$

Table 2. Determination of the kinetic parameters of some experimental DTA curves[6,7] by Curve fitting method. E_{BD} stands for the activation energy calulated by using Borchardt and Daniels method

Chemical reactions studied	E (KJmole^{-1})	n	A (s^{-1})	E_{BD} (KJmole^{-1})
$Ni(mpipz)_2(NCS)_2].2H_2O \rightarrow Ni(mpipz)_2(NCS)_2]$	143.9	1.5	7.83(16)	144.13
$Ca[(DMP)_2(MCA)_2 \rightarrow Ca[(DMP)(MCA)_2]$	35.0	1.0	82.35	35.02

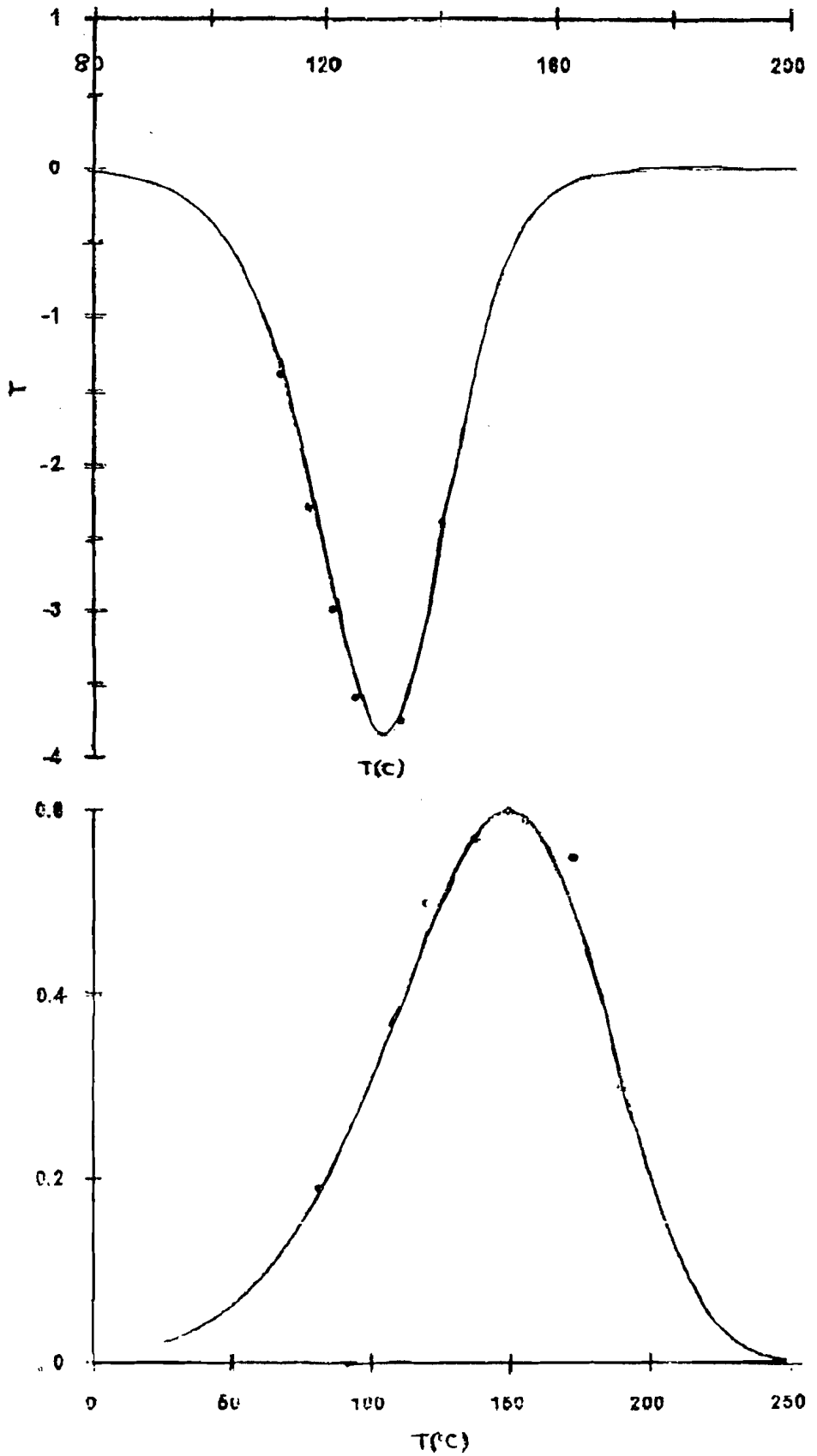
1
80
120
160
200
0
-1
-2
-3
-4
T
T(C)
0.6
0.4
0.2
0
0
50
100
150
200
250
T(°C)